PRINCIPLE AND IMPLEMENTATION OF VECTOR-BASED PHASOR MEASUREMENT UNIT ALGORITHM USING DELAY DEVICES

Suminori Nishie

PRIMO Signal Processing Laboratory
Kawana, Fujisawa, Kanagawa, 251-0015, Japan
snishie@mac.com

ABSTRACT

This paper proposes a novel Phasor Measurement Unit (PMU) algorithm for P and M class measurement using vector-based operation with originally designed pseudo-IQ signal translation using a delay device. A PMU is an essential equipment in the smart grid. However some technical difficulties with frequency measurement are still discussed. The presented algorithm in this paper aims to be a compact algorithm with implementations for breakthrough by 1) directly measuring the nominal frequency by using an F0 measurement method, 2) using vector product operation to calculate the phasor, and 3) not using DFT or the quadrature heterodyne method due to the difficult filter design requirements This paper also reports on the evaluation result based on IEEE Std C37.118.1, and the presented algorithm shows excellent frequency measurement, dynamic response, stability, and preciseness

Index Terms— PMU, IQ-signal, Instantaneous Frequency, Delay Device

1. INTRODUCTION

The phasor measurement unit (PMU) is the key equipment in the smart grid and its applications. The PMU monitors voltage and phasor information by specified report rate (F_s). However, the PMU algorithm currently has technical difficulties concerning the frequency measurement of dynamic waveforms [1]. In particular, the C37.118 requirement amendment [2] stated that a few requirements were achievable.

In particular, it was difficult to meet the mains frequency (f_0), rate of change of frequency (ROCOF), frequency error (FE), and ROCOF error (RFE) requirements with the latest hardware when the reference model provided in the standard was used . The main stream of frequency/phasor measurement methods are DFT-based or quadrature heterodyne. There are drawbacks with both. The frame length in DFT should fit the nominal frequency. The design of the low pass filter (LPF) in the quadrature heterodyne method as described in C.37.118 [3] to achieve out-of-band robustness is difficult. A DFT-based algorithm with fitting [4] shows higher accuracy; however, this implementation requires high performance FPGA(s).

This research aims to achieve precise frequency measurement in two cycles of single-phase input while complying with both P and M class requirements. The second purpose is that our algorithm can run on an ordinary PC and embedded software. To achieve the above purposes, we used vector product operation and introduced an F0 measurement method originally designed for acoustic signal processing [5]. If we can directly measure nominal mains frequency (50/60 Hz) without using three-phase inputs, the measurement of ROCOF can be improved, and most of the problems that we face can be solved.

The proposed algorithm in this paper consists of five units: 1) direct frequency measurement, 2) vector operation, 3) IQ-signal transform, 4) reference signal generator, and 5) averaging operation for miscellaneous purposes.

This paper firstly illustrates the algorithm and implementations on a PC, secondly shows the total vector error (TVE) evaluation based on the IEEE standard [3], and finally demonstrates excellent capability of frequency tracking by using a high ramp rate (Hz/s) in single-phase input and discontinuously changing the frequency of the input.

2. PRINCIPLE

This section describes the principle and processing diagram of the vector-based synchrophasor measurement. In this paper, we use normalised frequency. $F = \frac{f}{f_s}$, $\Omega = 2\pi F = 2\pi f/f_s = \Omega/f_s$, where f_s is the sampling frequency. The sampling interval $\Delta T = 1/f_s$. Let ϕ denote the phase angle or phase difference. In this paper, signals are described in a discrete system as explained in Eq. (1)

$$\begin{aligned} s_{(t)} &= A \cdot \sin(\omega t - \phi) \\ s_{[n]} &= A \cdot \sin(\omega(\Delta T n) - \phi) = A \cdot \sin(\Omega n - \phi) \\ where \quad \Omega &= 2\pi f/f_s = \omega/f_s = \omega \cdot \Delta T \end{aligned} \tag{1}$$

2.1. Signal Diagram and Overview

First of all, the system diagram is illustrated in Fig. 1. The amplitude/phasor information can be calculated by vector operation (dot, cross, and norm). The vector operation is per-

978-0-9928626-3-3/15/$31.00 ©2015 IEEE

formed by using IQ signals; the IQ translation is performed based on frequency information. The frequency is measured as the instantaneous frequency (IF) . The functions are explained below.

1. IF unit measures the instantaneous frequency using the delay operation, algorithm, and formula, which are described in section 2.2.
2. IQ unit translates the real single-phase signal to the IQ signal using one delay device. The author named this pseudo-IQ translation. The details are described in section 2.4.
3. Vector-op. calculates vector products (dot and cross) for phasor and amplitude by using the norm.
4. Reference oscillator provides reference quadrature signals to vector-op.

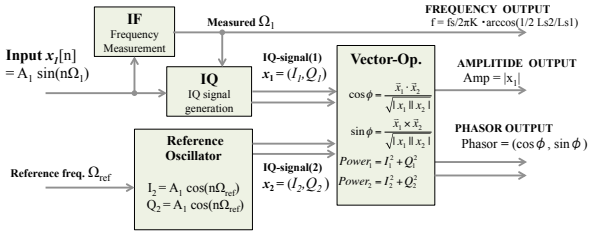

Fig. 1: Signal Processing Diagram

2.2. Instantaneous Frequency Measurement

This section describes a novel method for instantaneous frequency measurement by using a set of explicit functions, as described in Eq. (2). Note that f_s is the sampling frequency and K is the delay count in the unit. The implementation uses averaged values of Ls for more robustness. Lissajous' product Ls is explained in section 2.2.2. Note that four samples of input data are used to obtain the instantaneous frequency.

$$\begin{aligned} f_{[i]} &= \frac{f_s}{2\pi K} \arccos\left\{\frac{1}{2}\cdot\frac{Ls_{2[i]}}{Ls_{1[i]}}\right\} \\ Ls_1[i] &= s_{[i-K/2]}s_{[i-3K/2-1]} - s_{[i-K/2-1]}s_{[i-3K/2]} \\ Ls_2[i] &= s_{[i]}s_{[i-2K-1]} - s_{[i-1]}s_{[i-2K]} \end{aligned} \quad (2)$$

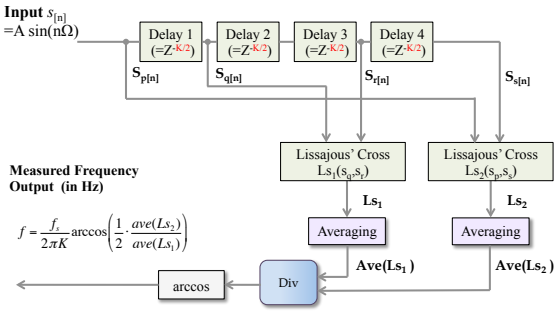

Fig. 2: Frequency-Measurement Unit

2.2.1. Derivation of Formula

In this subsection, we explain the derivation of Eq. (2). The idea of the formula comes from the traditional Lissajous' figure. Section 2.2.2 describes the idea of the *Lissajous' product*. Section 2.2.3 describes how to measure phase shift using the *Lissajous' Product*. Section 2.2.4 describes the phase shift on a delay device. Section 2.2.5 derives the final equation.

2.2.2. Lissajous' Figure

Figure 3 shows the Lissajous' figure and the partial movement. Let $Ls(x, y)$ denote *the Lissajous' product* defined by Eq. (3) Note that the small triangle area ΔS in Fig. 3 equals $1/2Ls$.

$$Ls(x_n, y_n) = x_{n-1} \cdot y_n - x_n \cdot y_{n-1} \quad (3)$$

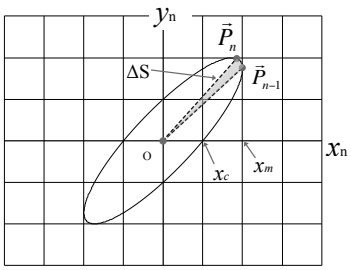

Fig. 3: Lissajous' Figure

2.2.3. Phase Shift Calculation

The author has presented Eq. (4) for phase shift calculation [6]. Eq. (4) means that the phase difference between signal x_n, y_n can be calculated by using the above Lissajous' product and given frequency $\Omega(= 2\pi f/f_s)$. This subsection describes the derivation of Eq. (4).

$$\sin\phi_c = \frac{L_s(x_n, y_n)}{AB\sin\Omega} \quad (4)$$

(1) Signal Assumption

First, assuming $x(t) = A\sin(\omega t)$, $y(t) = B\sin(\omega t - \phi_c)$ as the Lissajous' figure traces indicate in Eq. (5).

$$\begin{aligned} x_1 &= x_{n-1} = A\sin(\Omega(n-1)) \\ y_1 &= y_{n-1} = B\sin(\Omega(n-1) - \phi_c) \\ x_2 &= x_n = A\sin(\Omega n) \\ y_2 &= y_n = B\sin(\Omega n - \phi_c) \\ \vec{P1} &= (x_1, y_1) \quad , \vec{P2} = (x_2, y_2) \end{aligned} \quad (5)$$

The area of the triangle ΔS is obtained by Eq.(6)

$$\Delta S = \frac{1}{2}(\vec{P_1} \times \vec{P_2}) = \frac{1}{2}(x_1y_2 - x_2y_1) \quad (6)$$

(2) ΔS transform

Second, Eq. (6) is transformed into Eq. (7). To simplify, $\sin X \sin Y = \frac{1}{2}\{\cos(X-Y) - \cos(X+Y)\}$ is used.

$$\begin{aligned} \Delta S &= \frac{1}{2}(x_1y_2 - x_2y_1) \\ &= \tfrac{1}{2}AB\{\sin(\Omega(n-1)) \cdot \sin(\Omega n - \phi_c)\} \\ &\quad -\tfrac{1}{2}AB\{\sin(\Omega n) \cdot \sin(\Omega(n-1) - \phi_c)\} \\ &= \tfrac{1}{4}AB\{\cos(-\Omega + \phi_c) - \cos(\Omega(2n-1) - \phi_c)\} \\ &- \tfrac{1}{4}AB\{\cos(\Omega + \phi_c) - \cos(\Omega(2n-1) - \phi_c)\} \\ &= \tfrac{1}{4}AB\{\cos(-\Omega + \phi_c) - \cos(\Omega + \phi_c)\} \end{aligned} \quad (7)$$

Then, using $\cos X - \cos Y = -2\sin(\frac{X+Y}{2})\sin(\frac{X-Y}{2})$, Eq. (7) is simplified. Next, Eq. (8) is derived.

$$\begin{aligned}\Delta S &= \tfrac{1}{4}AB\{\cos(-\Omega+\phi_c)-\cos(\Omega+\phi_c)\}\\ &= -\tfrac{1}{2}AB\{\sin(\phi_c)\cdot\sin(-\Omega)\}\\ &= \tfrac{1}{2}AB\{\sin(\phi_c)\cdot\sin(\Omega)\}\end{aligned} \quad (8)$$

Note that $\Delta S = \frac{1}{2}Ls(x,y)$; therefore,

$$\sin\phi_c = \frac{L_s(x,y)}{AB\sin\Omega} \quad (9)$$

Eq. (4) was derived.

2.2.4. *Phase Difference on a Delay Device*

A Delay device (delay = K, sampling frequency f_s, $\Delta T = 1/f_s$) causes phase difference $\phi = K\Omega$ using normalised frequency Ω, as shown in Eq. (10).

$$\begin{aligned}\sin(\omega(t+K\Delta T)) &= \sin(\omega t + K\omega\Delta T)\\ &= \sin(\omega t + K\Omega)\end{aligned} \quad (10)$$

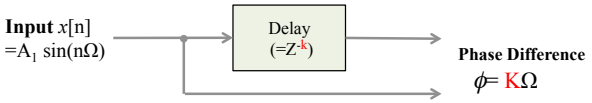

Fig. 4: Phase Difference on a Delay Device

2.2.5. *Instantaneous Frequency by Two Delay Device*

This section shows the final step of deriving Eq. (2). We use the phase shift on a delay device as explained above. The phase difference ϕ_1 on Delay1 (shift = K) and ϕ_2 on Delay2 (shift = 2K) are considered. Figure 5 shows an implementation example of preparing a K and 2K delay. The phase differences of $\phi_1$and ϕ_2 are described in Eq. (11),(12).

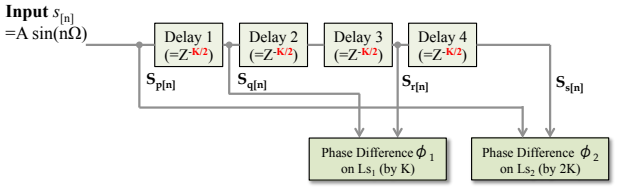

Fig. 5: Phase Shift ϕ_1, ϕ_2 on Two Delay Devices

$$\sin\phi_1 = \sin K\Omega = \frac{Ls_1}{A^2\sin\Omega} \quad (11)$$

$$\sin\phi_2 = \sin 2K\Omega = \frac{Ls_2}{A^2\sin\Omega} \quad (12)$$

Here, by combining Eq. (11) and Eq. (12) and by using $\sin 2x = 2\cos x\sin x$, Eq. (13) is derived.

$$\begin{aligned}\frac{\sin 2K\Omega}{\sin K\Omega} &= \frac{Ls_2}{Ls_1} = 2\cos K\Omega\\ \Omega &= \frac{1}{K}\arccos\left(\frac{1}{2}\frac{Ls_2}{Ls_1}\right)\\ f &= \frac{f_s}{2\pi K}\arccos\left(\frac{1}{2}\frac{Ls_2}{Ls_1}\right)\end{aligned} \quad (13)$$

2.3. Vector Operation

The vector operation calculates the amplitude, phasor, and frequency. The phasor can be obtained by using the vector product and Eq. (14) (Fig. 6). Note that the input signals must be IQ signals.

$$\cos\phi = \frac{\vec{x_1}\cdot\vec{x_2}}{|\vec{x_!}||\vec{x_2}|}, \quad \sin\phi = \frac{\vec{x_1}\times\vec{x_2}}{|\vec{x_1}||\vec{x_2}|} \quad (14)$$

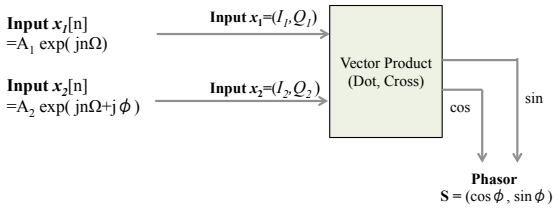

Fig. 6: Vector Operation

2.4. IQ-Signal Generation

Vector operation was explained in the previous section. However, IQ signals are mandatory. This section illustrates our simple approach to generate IQ signals (Fig. 7). Transformation is described in Eq. (15). The principle is the phase difference on a delay device described in section 2.2.4. To generate accurate $\pi/2$ phase shift, linear composition with a_0, a_1 is applied. a_0, a_1 are calculated as shown in Fig. 8.

$$\begin{aligned}a_0 &= \tan(K\Omega - \frac{\pi}{2}), \quad a_1 = \frac{1}{\cos(K\Omega-\frac{\pi}{2})}\\ I_n &= x_n\\ Q_n &= a_0\cdot x_x + a_1\cdot x_{n-K}\end{aligned} \quad (15)$$

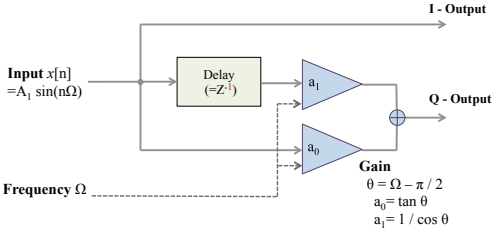

Fig. 7: Pseud-IQ Signal Generation

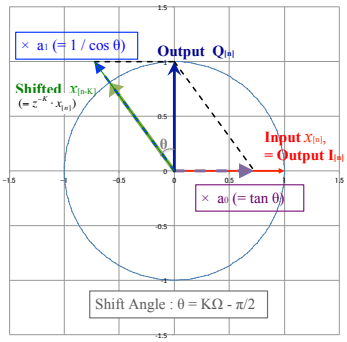

Fig. 8: Vector chart to define a_0 , a_1

2.5. Averaging

The averaging operation is used in this system. This section shows the optimised moving average method to reduce the calculation amount. In general, averaging can be described in the z-domain as Eq. (16).

$$H_{ave} = \frac{1}{N}\{1 + z^{-1} + z^{-2} + ... + z^{-(N-1)}\} \quad (16)$$

This can be translated as:

$$H_{ave} = \frac{1}{N}\left\{\frac{1 - z^{-N}}{1 - z^{-1}}\right\} \quad (17)$$

Eq. (17) indicates that the operation requires one integration, one subtraction, and one division as specified by count N. The number of additions is less than that of Eq. (16). Figure 9 shows the signal processing diagram.

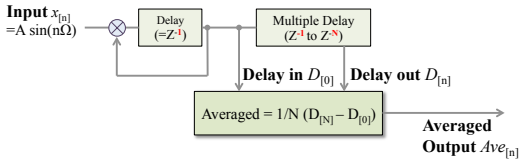

Fig. 9: Averaging Operation

3. IMPLEMENTATION

The algorithm was implemented on a PC with audio IO, WAV file IO, and software-emulated signal generation.

- PC: iMac (Intel Core 2 Duo, 2.66 GHz)
- OS: Windows 7, Visual C++ 2010, native programming with GDI control. No MFC is used.
- ADC: f_s = 44100 Hz, general audio interface.
- Max 8 CH can be processed.
- Result: averaged in $1/Fs$ sec (tunable).
- Time Window: $2/f_0$ (40 msec for 50 Hz)

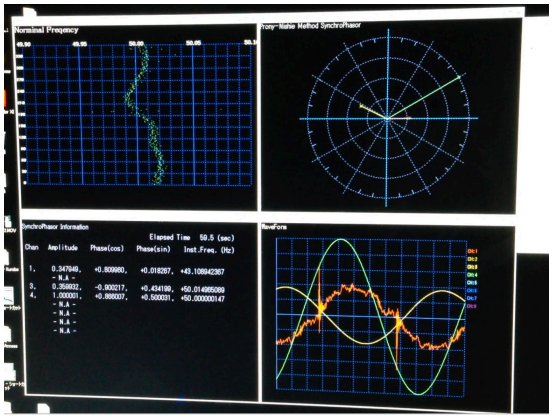

Fig. 10: Screen Shot of Prototype Software (Upper Left: Mains Frequency),(Upper Right: Phasor), (Lower Left: Numerical Result),(Lower Right: Waveforms)

4. EVALUATION

This section describes the evaluation results. In this evaluation, in particular, we focus on frequency resolution and dynamic response of frequency movement in input signals. To evaluate the dynamic response, frequency tracking examination by high frequency change rate was performed.

4.1. TVE

The TVE results are shown in Table 1. Pure sinusoid waves were used. Higher reporting rates (F_s) were intentionally examined to show the quick processing cycle.

Table 1: TVE Evaluation (Pure Signal)

Fs(report rate)		10	50	100	200
Freq. (Hz)	45.0	0.4168	0.4168	0.4168	0.4168
	49.5	0.0082	0.0082	0.0082	0.0082
	49.9	0.0014	0.0014	0.0014	0.0014
	50.0	0.0001	0.0001	0.0001	0.0001
	50.1	0.0015	0.0015	0.0015	0.0015
	50.5	0.0082	0.0082	0.0082	0.0082
	55.0	0.4168	0.4168	0.4168	0.4168

Unit per cent. Using pure sinusoid wave

4.2. Linear Frequency Ramp Test

Figure 11 shows the results of the linear frequency ramp tracking test. The standard is described in Table 7 of IEEE Std C.37.118 [3]. The low change rate of 1 Hz/sec and the high change rate of 100 Hz/sec were examined.

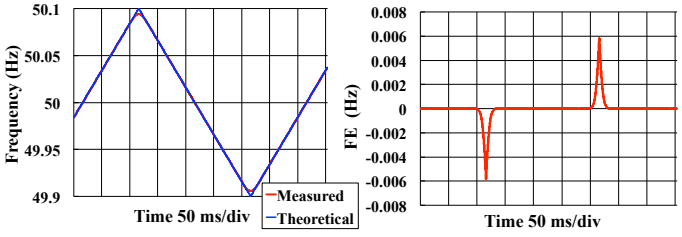

(a) Frequency (b) FE

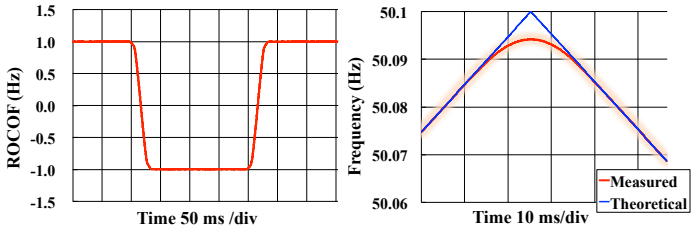

(c) ROCOF (d) Transient

Fig. 11: Linear Frequency Ramp Tracking Test (Low Rate = 1.0Hz/sec)

4.3. Step Frequency Change Test

Figure 13 shows the results of step frequency change tracking. The technical information is described in Annex B in IEEE Std C.37.118 [3]. The step frequency change causes transient behaviour; however, this disappears in several decades

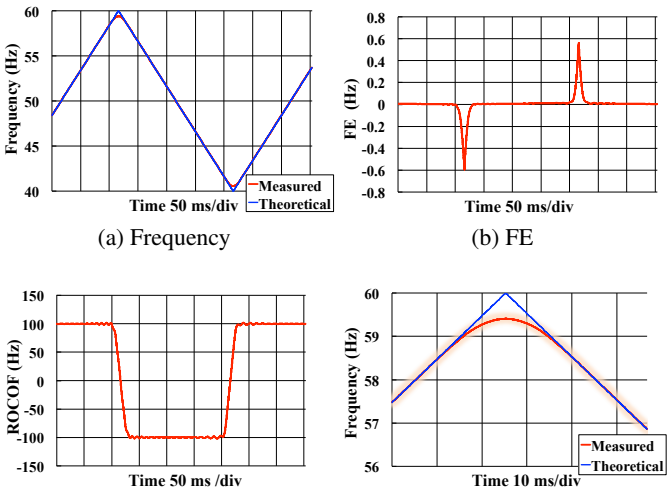

(a) Frequency (b) FE

(c) ROCOF (d) Transient

Fig. 12: Linear Frequency Ramp Tracking Test (High Rate = 100Hz/sec)

of msec on our algorithm. The step frequency change causes phase shift. The measured phase angle was consistent with the theoretical value.

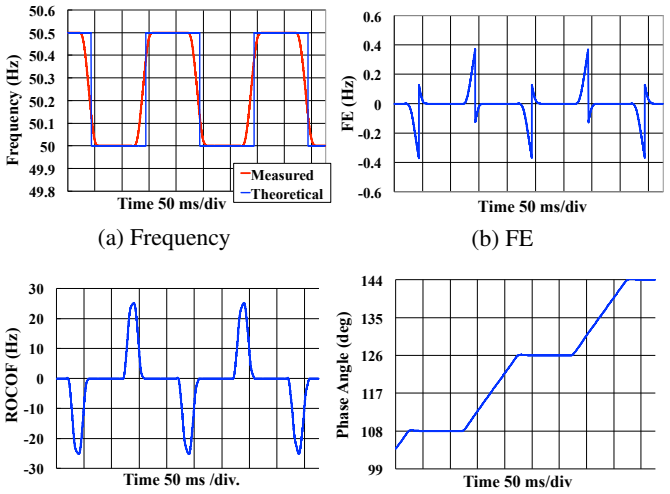

(a) Frequency (b) FE

(c) ROCOF (d) Phase Shift by Step Frequency Change

Fig. 13: Step Frequency Change Tracking Test (± 0.5Hz)

4.4. Mains Frequency Measurement

Figure 14 shows mains frequency tracking in Kansai Electric Power Company (KEPCO) measured in Nomi City, Ishikawa prefecture. The waveform was monitored indirectly by static induction from 275 kV lines without transform (VCT). Small movements with different periods are observed.

5. SUMMARY OF EVALUATION

The TVE evaluation satisfies the steady-state requirements in C37.118. The ramp/step frequency test results show the pre-

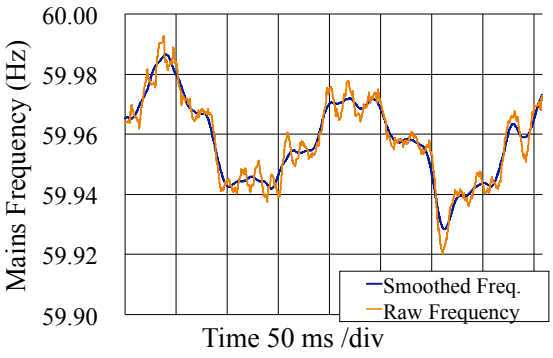

Fig. 14: Measurement of Mains Frequency of KEPCO Japan

sented algorithm has excellent transient response in a short period and preciseness. The implemented SW can directly measure mains frequency as proven by the field test.

6. CONCLUSION

A novel algorithm without DFT and compact implementation of synchrophasor was proposed. Excellent capability of frequency tracking by the presented algorithm was demonstrated.

7. REFERENCES

[1] Kamwa, Innocent, S. R. Samantaray, and Geza Joos. "Wide frequency range adaptive phasor and frequency PMU algorithms." Smart Grid, IEEE Transactions on 5.2 (2014): 569-579.

[2] IEEE Standard for Synchrophasors for Power Systems Amendment 1: Modification of Selected Performance Requirements, IEEE Std. C37.118.1a, 2014.

[3] IEEE Standard for Synchrophasors for Power Systems, IEEE Std. C37.118.1, 2011.

[4] Paolone, Mario, Alberto Borghetti, and Carlo Alberto Nucci. "A synchrophasor estimation algorithm for the monitoring of active distribution networks in steady state and transient conditions." Proc. of the 17th Power Systems Computation Conference (PSCC 2011), Stockholm, Sweden. 2011.

[5] Nishie, Suminori, and Masato Akagi. "Instantaneous Frequency Measurement Method Using Phase Shift on Delay Devices." (Japanese) IEICE, vol. 113, no. 349, EA2013-93, pp. 31-36, 2013.

[6] Nishie, Suminori, and Masato Akagi. "Acoustic sound source tracking for a moving object using precise Doppler-shift measurement." Signal Processing Conference (EUSIPCO), 2013 Proceedings of the 21st European. IEEE, 2013.